Enhancing transmitarray bandwidth at 300 GHz via combined spatial point-focusing and far-field phase profiles

Marc Zhan, David Demmer, Antonio Clemente

▶ **To cite this version:**

Marc Zhan, David Demmer, Antonio Clemente. Enhancing transmitarray bandwidth at 300 GHz via combined spatial point-focusing and far-field phase profiles. URSI Gaas - XXXVIth URSI General Assembly and Scientific Symposium, URSI, Aug 2026, Cracovie, Poland. ⟨cea-05570561⟩

HAL Id: cea-05570561

https://cea.hal.science/cea-05570561v1

Submitted on 27 Mar 2026

HAL is a multi-disciplinary open access archive for the deposit and dissemination of scientific research documents, whether they are published or not. The documents may come from teaching and research institutions in France or abroad, or from public or private research centers.

L'archive ouverte pluridisciplinaire **HAL**, est destinée au dépôt et à la diffusion de documents scientifiques de niveau recherche, publiés ou non, émanant des établissements d'enseignement et de recherche français ou étrangers, des laboratoires publics ou privés.

Distributed under a Creative Commons CC BY-NC 4.0 - Attribution - Non-commercial use - International License

URSI GASS 2026, Krakow, Poland, 15 – 22 August 2026

Enhancing Transmitarray Bandwidth at 300 GHz via Combined Spatial Point-Focusing and Far-Field Phase Profiles

Marc Zhan, David Demmer, and Antonio Clemente
CEA, Leti, Université Grenoble Alpes, Grenoble, France

Abstract

This paper proposes a hybrid synthesis method combining spatial point-focusing beamforming and far-field phase profiling to enhance the operating bandwidth of transmitarrays. The phase distribution required for a broadband fixed-beam operation is derived based on a numerical model of the transmitarray, and the impact of key design parameters on antenna performance is systematically evaluated. The proposed approach demonstrates significant bandwidth improvement while limiting peak-gain degradation to 1.7–3.4 dB, and its effectiveness is validated through comparison with conventional techniques, such as feed focal-distance adjustment for plane-wave illumination approximation.

1 Introduction

A transmitarray (TA) is a spatially fed antenna architecture that has attracted significant interest for a wide range of applications, ranging from real-time electronically steerable beamforming [1] to fixed-beam, high-gain point-to-point links [2, 3]. Owing to their low cost, reduced complexity, and low power consumption, TAs represent an appealing alternative to classical phased arrays. Nevertheless, TAs inherently suffer from non-uniform aperture illumination in both amplitude and phase, which limits their broadband performance. When combined with the frequency-invariant phase response of the unit cells (UCs), this non-uniform illumination induces a frequency-dependent deformation of the radiated beam, even for broadside operation. In particular, the use of a constant phase-shift law optimized at a single design frequency results in a reduced operational bandwidth, as reported in [4]. Furthermore, under beam-steering conditions, this frequency-dispersive behavior causes a progressive shift of the main beam direction with frequency, known as beam squint, which further degrades wideband performance.

Most state-of-the-art solutions address these limitations either by increasing the focal distance to alleviate aperture illumination non-uniformity or by employing complex multilayer unit-cell architectures to compensate for frequency dispersion [5]. While adjusting the feed position and focal distance can improve the bandwidth by enabling a more favorable gain–bandwidth trade-off [2], such improvements are typically achieved at the expense of a significant peak-gain reduction. These drawbacks motivate the development of alternative synthesis strategies capable of delivering improved bandwidth without severe gain penalties, particularly for fixed-beam sub-THz backhaul applications.

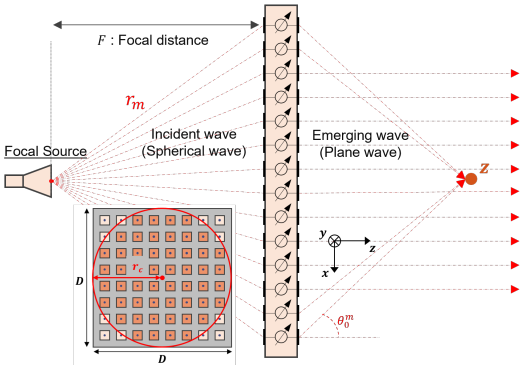

Figure 1. TA System Modeling

In this context, this work investigates a phase-only synthesis approach based on a mixed far-field and point-focusing (mFF–PF) beamforming scheme. The proposed method introduces a parametric phase profile, which is analyzed using a numerical TA model. An optimized phase distribution is then derived and employed to quantitatively assess the achievable performance, through comparison with conventional synthesis techniques and with measured performance indicators from experimental demonstrations.

The remainder of this paper is organized as follows. Section 2 presents the TA modeling framework. Section 3 describes both the conventional and proposed synthesis approaches. Section 4 evaluates the achievable performance and benchmarks the proposed scheme. Finally, conclusions are drawn in Section 5.

2 Ray-Tracing Model for Transmitarrays

We assume a square TA aperture of $M \times M$ elements, lying $z = 0$ plane and centered at the origin of the coordinate system. The TA is illuminated by a feed whose phase center is in $(0, 0, -F)$ where F is the focal distance. The UCs are synthesized as pairs of receiving (Rx) and transmit (Tx) elements coupled by a phase shifter. A perfect power transmission from Rx and Tx elements, *i.e.* a lossless power propagation through each UC.

The directivity of the feeding source D_{FS} and each UC an-

tenna (same for both *Rx* and *Tx*) D_{UC} are expressed as follows [6, 7]:

$$D_{FS}(\theta) = 2(p+1)\cos^p(\theta) \quad (1)$$

$$D_{UC}(\lambda,\theta) = \frac{4\pi A_{phy}}{\lambda^2}\cos(\theta) \quad (2)$$

where the directivity increases with the order p, $A_{phy} = \lambda_c^2/4$ is the UC's area and λ indicates the wavelength at the operation frequency.

By assuming the far-field (FF) propagation between the FS and the *Rx* element for the m-th UC, the propagation channel, h_m, can be expressed as [7]:

$$h_m(\lambda) = \sqrt{D_{FS}(\theta_m)\cdot D_{UC}(\lambda,\theta_m)}\frac{\lambda}{4\pi r_m}e^{-j\frac{2\pi}{\lambda}r_m} \quad (3)$$

where $r_m = \sqrt{F^2+x_m^2+y_m^2}$ denotes the distance between the FS and the m-th UC, and θ_m represents the elevation angle between the phase centers of the FS and the m-th UC. Expression (3) characterizes the illumination law of the TA. One can observe that the incident phase and amplitude are function of the wavelength and space (*i.e.* UC location).

Finally, the radiation pattern of the TA is computed by sumperimposing the contribution of each UC

$$g(\lambda,\theta,\phi) = \left|\sum_m \sqrt{D_{UC}(\lambda,\theta)}h_m(\lambda)e^{j(\beta_m+\frac{2\pi}{\lambda}(ux_m+vy_m))}\right|^2 \quad (4)$$

where β_m is the phase shift applied at the m-th UC, $(u,v) = (\sin\theta\cos\phi, \sin\theta\sin\phi)$ and (x_m, y_m) denote the position in the xy-plane of the m-th UC.

3 Phase Profile Synthesis

We now present two methods to derive the phase distribution of the TA. In all cases, a continuous phase-shift in the range 0-2π is considered for each UC with a constant phase shift in the band [8].

3.1 Far-Field Canonical Phase Profile

Under narrowband approximation, the phase distribution is optimized to steer a beam at a given direction. In particular for broadside beam, the phase of the m-th UC is given by [7]

$$\beta_m = \frac{2\pi}{\lambda_c}r_m \quad (5)$$

Typically, the focal distance is selected to maximize the peak gain [9]. For wideband TAs, it is possible to adapt the focal distance to achieve a more favorable trade-off between gain and operational bandwidth [2].

3.2 Proposed Mixed Far-Field and Point-Focusing Phase Profile

We propose to divide the TA aperture into two distinct subarrays using a circle of radius r_c, as shown in Figure 1. The UCs inside r_c aims at compensating the incident phase at central frequency as described in the previous section,

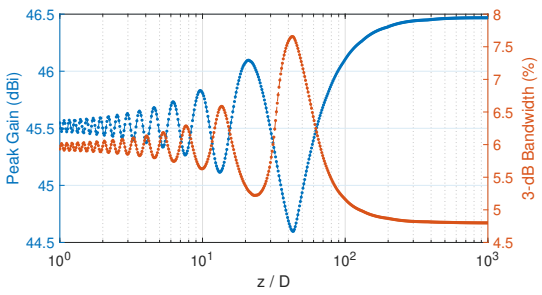

Figure 2. Achievable trade-offs between peak-gain and 3-dB bandwidth for the proposed mFF-PF with $r_c = D/2$ applied to the 140×140 TA (F/D=0.47).

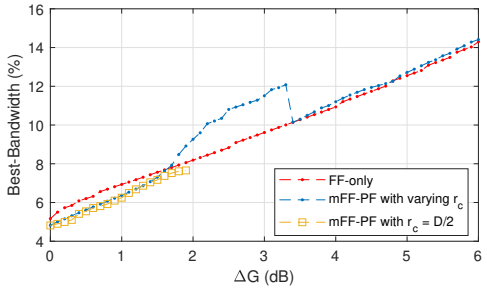

Figure 3. Bandwidth for Minimal Gain-Loss.

while the UCs outside of the circle also perform point-focusing toward a virtual point located at $(0,0,z)$ (with $z>0$). The idea behind point-focusing is to limit the effects of frequency dispersion. Indeed, frequency components above and below the carrier frequency f_c cause beam deviations in opposite directions, respectively toward the outward and inward from the desired direction. Accordingly, the PF method compensates for the outward beam deviation at higher frequencies, at the price of reduced gain at the carrier frequency.

This approach depends on two parameters: the circle radius r_c and the focal point distance z. The expression of the phase shift of the m-th UC is thus

$$\beta_m = \begin{cases} \frac{2\pi}{\lambda_c}r_m, & x_m^2+y_m^2 \le r_c^2 \\ \frac{2\pi}{\lambda_c}\left(r_m + \frac{x_m^2+x_m^2}{\sqrt{x_m^2+y_m^2+z^2}}\right), & \text{otherwise.} \end{cases} \quad (6)$$

It is interesting to observe that the proposed method is a generalization of the FF phase profile. Indeed, for $r_c > \sqrt{2}D/2$, the circle totally encloses the lens of UCs and therefore the proposed method is reduced to FF beamforming. Similarly, for $r_c < \sqrt{2}D/2$, when $z\to\infty$ the proposed method is reduced to FF beamforming.

4 Simulation Results

A 140×140 broadside TA operating at carrier frequency $f_c = 300GHz$ is considered. The TA period is equal to $\lambda_c/2$. The FS is a pyramidal horn antenna whit a gain of 10 dBi (*i.e.*, an antenna order $p=4$). The gain-maximized configuration achieving 46.5 dBi gain and 4.8% relative 3-dB

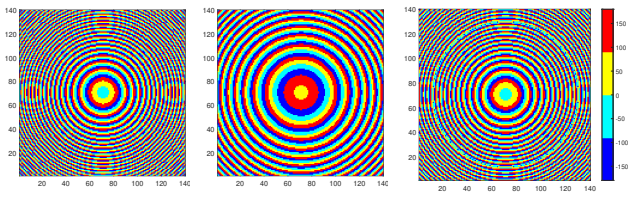

(a) Reference **(b)** FF-only **(c)** mFF-PF

Figure 4. Phase Profiles of the Reference and 3 dB peak Gain Loss FF-only and mPF-FF configurations.

bandwidth for $F/D = 0.47$ (according the considered wide-band model) is used as reference.

4.1 Evaluation of the Proposed Solution

We now evaluate the achievable performance of the proposed scheme. For sake of compactness, we assume in the proposed study that the focal distance is set to $F/D = 0.47$. Figure 2 gives the peak gain and corresponding 3-dB bandwidth as function of the focusing distance z for a fixed circle radius $r_c = D/2$ (for illustration). As expected, the maximum peak gain is achieved for $z \to \infty$. Then, the system provides different trade-off levels depending on the distance z. For instance, maximum 3-dB bandwidth is achieved for $z = 43D$ at the price of a peak gain reduction of 1.9 dB. Based on this, we can evaluate the best bandwidth as function of the peak gain penalty with respect to the maximized gain 46.5 dBi. It leads to the yellow curve depicted in Figure 3. We can now extend this result by evaluating the performance for any circle radius $r_c \in [0, \sqrt{2}D/2]$. We can thus evaluate the maximum bandwidth as function of the peak gain penalty for any configuration (r_c, z) which leads to the blue curve in Figure 3. The performance provided by FF-only scheme by varying the focal distance is also given for comparison. Regarding the FF-only phase profile, the best bandwidth performance is achieved by enlarging the focal distance (as it tends to a better uniform phase illumination law). The bandwidth comes at the price of a peak-gain penalty caused by increased spillover losses. The mFF-PF method outperforms the FF-only approach for a gain loss between 1.7 and 3.4 dB. Therefore, the 3 dB gain penalty configuration will be considered for the benchmark.

4.2 Performance Evaluation

Table 1 provides the obtained configurations and evaluations of key performance indicators. The numerical results are also compared with state-of-the-art high-gain sub-THz antennas, whose results are based on real measurements.

The obtained phase profiles, rounded to $\pi/2$ for readability, are shown in Figure 4. The FF-only phase profile exhibits less phase discontinuities than the reference case, thanks to a better uniform phase illumination. In contrast, the mFF-PF phase profile splits the array into two, keeping the inner UCs identical to the reference and directing the outer UCs toward the virtual focusing point $(0, 0, z)$.

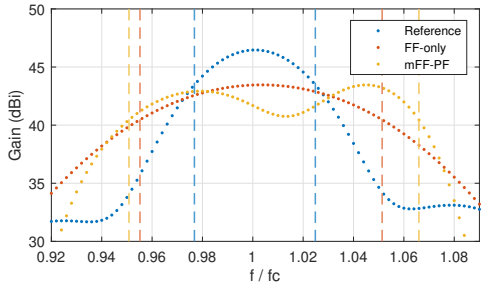

Figure 5. Gain versus Frequency

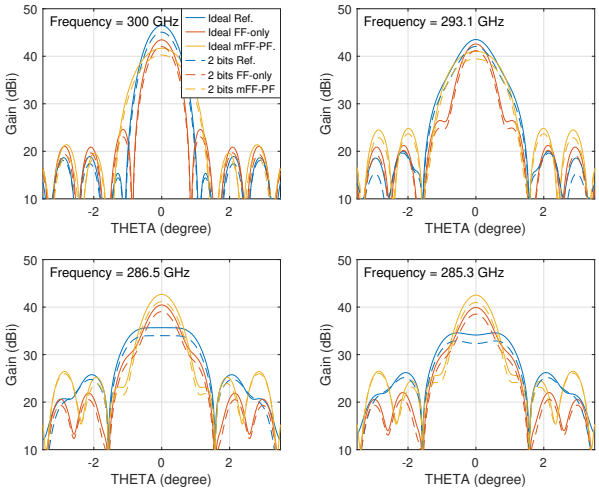

Figure 6. Radiation Pattern ($\phi = 0$) for Different Phase Resolutions and Methods (Reference, FF-only, mFF-PF)

Figure 5 depicts the gains provided by the different configurations. The aperture efficiency is defined as the ratio between the achievable peak gain and the theoretical directivity of a uniformly illuminated aperture (in amplitude and phase) having the same physical dimensions $D \times D$ as the array. The corresponding 3-dB bandwidth are depicted by vertical dashed lines. We can observe that the proposed mFF-PF phase profile forms two local maxima for the gain response and no maximum at $f = f_c$. The peak gain and bandwidth are selected to maximize the bandwidth around the center frequency. In addition, the peak aperture efficiency decreases from 71.9% to 35.6% and 33.3% for the FF-only and mFF-PF approaches, respectively. It is mainly due to the 3 dB gain reduction we considered.

Figure 6 depicts the radiation patterns evaluated at different frequencies. The bandwidth enlargement is achieved at the price of increased SLL at the carrier frequency f_c. The SLL increases from -27 dB to -19 dB for FF-only approach and to -20 dB for mFF-PF approach under both ideal and 2-bit phase quantized conditions. Furthermore, 2-bit phase quantization results in a peak gain loss of 1.4 dB. It motivates us to conduct a more comprehensive investigation of the impact of phase quantization on radiation performance that will be addressed in future work.

Compared with other state-of-the-art high-gain sub-THz experimental TAs, the point-focused method demonstrates

Table 1. Synthesis of 3-dB gain-penalty configurations and achieved performance in comparison with experimental prototypes.

Method	Reference	FF-only	mFF-PF	[2]	[3]	[1]
Frequency (GHz)	300	300	300	280	140	200
Source gain [dBi]	10.0	10.0	10.0	10.0	25.5	22.0
D/λ_c	70	70	70	70 (at 300 GHz)	94	15
F/D	0.47	1.26	0.47	0.60	1.69	1.78
r_c/(D/2) : z/D	$>\sqrt{2}:\infty$	$>\sqrt{2}:\infty$	0.84 : 29.5	$>\sqrt{2}:\infty$	$>\sqrt{2}:\infty$	$>\sqrt{2}:\infty$
Peak Gain [dBi]	46.5	43.5	43.5	43.3	44.3	29.2
3dB- Bandwidth	4.8%	9.6%	11.5%	6.0%	6.4%	19.1%
Peak Aperture Eff.	71.9%	35.9%	33.3%	39.0%	24.1%	35.0%
SLL [dB]	-27	−19	−20	−17	−30	−18

superior bandwidth performance with a short focal distance fixed to $F/D = 0.47$. Indeed, the 3-dB bandwidth is nearly twice that reported in [2] and [3] while providing similar or even greater peak gains. It seems worth noticing that the TA in [1] exhibits a larger relative bandwidth of 19% thanks to its small lens size, $D/\lambda = 16$, and greater focal distance, $F/D = 1.67$. Consequently, its achievable gain is significantly lower than the other designs. Finally, it is important to note that the performance provided by the numerical ray-tracing model is optimistic compared to experimental measurements, mainly because the propagation through the lens is assumed to be ideal.

5 Conclusion

The proposed mFF–PF phase profiling achieves improved trade-offs between peak gain and bandwidth while maintaining a fixed focal distance. These results could be further extended by simultaneously adapting the focal distance. Moreover, the numerical results presented in this paper are somewhat optimistic compared to measurements of experimental prototypes. Nevertheless, the bandwidth improvements offered by the proposed scheme remain promising and warrant validation under more practical conditions, such as phase quantization and realistic full-wave simulations.

6 Acknowledgements

This work was supported by the French National Research Agency through project France 2030 titled NF-SYSTERA under grant agreement ANR-22-PEFT-0006.

References

[1] L.-Z. Song, T. Zhang, J.-X. Lai, Y. Yang, and J. Du, "A 180-GHz to 220-GHz wideband transmitarray with wide-angle beam steering for intersatellite communications," *IEEE Transactions on Antennas and Propagation*, vol. 72, no. 1, pp. 950–955, 2024.

[2] O. Koutsos, F. Foglia Manzillo, M. Caillet, R. Sauleau, and A. Clemente, "Experimental Demonstration of a 43-dBi Gain Transmitarray in PCB Technology for Backhauling in the 300-GHz Band," *IEEE Transactions on Terahertz Science and Technology*, vol. 13, no. 5, pp. 485–492, 2023.

[3] D. Seo, H. Kim, S. Oh, J. Kim, and J. Oh, "Ultrathin High-Gain D-Band Transmitarray Based on a Spatial Filter Topology Utilizing Bonding Layer Effect," *IEEE Antennas and Wireless Propagation Letters*, vol. 21, no. 10, pp. 1945–1949, 2022-10-01.

[4] F. Diaby, A. Clemente, L. Di Palma, L. Dussopt, and R. Sauleau, "Impact of phase compensation method on transmitarray performance," in *11th European Conference on Antennas and Propagation (EUCAP)*, 2017, pp. 3114–3118.

[5] L. Wen, S. Gao, Q. Luo, W. Hu, B. Sanz-Izquierdo, C. Wang, and X.-X. Yang, "Wideband Transmitarray Antenna Using Compact 2-bit Filtering Unit Cells," *IEEE Transactions on Antennas and Propagation*, vol. 71, no. 10, pp. 8344–8349, 2023.

[6] E. Plaza, G. Leon, S. Loredo, and F. Las-Heras, "A Simple Model for Analyzing Transmitarray Lenses," *IEEE Antennas and Propagation Magazine*, vol. 57, no. 2, pp. 131–144, 2015.

[7] A. Tummolo, O. Koutsos, F. Foglia Manzillo, A. Clemente, and R. Sauleau, "A Comparative Study on Ray-Tracing and Physical-Optics Methods for the Analysis of Transmitarray Antennas," in *19th European Conference on Antennas and Propagation (EuCAP)*, 2025, pp. 1–5.

[8] F. Diaby, A. Clemente, L. Di Palma, L. Dussopt, and R. Sauleau, "Impact of phase compensation method on transmitarray performance," in *11th European Conference on Antennas and Propagation (EUCAP)*, 2017, pp. 3114–3118.

[9] H. Kaouach, L. Dussopt, J. Lanteri, T. Koleck, and R. Sauleau, "Wideband Low-Loss Linear and Circular Polarization Transmit-Arrays in V-Band," *IEEE Transactions on Antennas and Propagation*, vol. 59, no. 7, pp. 2513–2523, 2011.